Infrared Spectra of the Novel Sn_2H_2 Species and the Reactive $SnH_{1,2,3}$ and $PbH_{1,2,3}$ Intermediates in Solid Neon, Deuterium, and Argon

Xuefeng Wang, Lester Andrews,* George V. Chertihin, and P. F. Souter

Department of Chemistry, University of Virginia, P.O. Box 400319, Charlottesville, Virginia 22904-4319

Received: March 14, 2002; In Final Form: April 5, 2002

Laser-ablated Sn atoms and H_2 molecules in excess neon and argon react during condensation to produce $SnH_{1,2,3,4}$ as identified from infrared spectra with D_2 and HD substitution, and from agreement with frequencies calculated by density functional theory. The novel ditin species Sn_2H_2 is also formed in further reactions. The $PbH_{1,2,3}$ intermediates are produced in analogous experiments. All four tin deuterides and the first three lead deuterides are observed in pure deuterium. Evidence is presented for the photosensitive MH_3^- and MH_2^- anions formed through electron capture processes.

Introduction

Plumbane, the lead analogue of methane, is said to be formed in traces when Mg−Pb alloys are hydrolyzed by acid, but its existence is doubted.[1] However, early investigation found the mass spectrum and cracking pattern of PbH_4 using this preparation,[2] and recent work obtained the gas-phase infrared spectrum of plumbane formed by $NaBH_4$ reduction of $Pb(NO)_2$ solution.[3] There is considerable theoretical interest in PbH_4 owing in part to relativistic effects on the bonding outlined in the early work of Pyykkö.[4] More recent calculations of Schwerdtfeger et al., Kaupp and Schleyer, and Dyall et al. show that the average bond energy in PbH_4 is slightly larger than that in PbH_2, but that PbH_4 decomposition to PbH_2 and H_2 is an exothermic process.[5−9] Stannane, on the other hand, is more stable, and its decomposition is endothermic.[9] Other workers have also investigated PbH_4 computationally and compared PbH_2 and PbH_4.[7,10−13] The theoretical work shows that PbH_4 will not form in the cold reaction of PbH_2 and H_2 although the analogous route is proposed for the formation of ZrH_4 and HfH_4 in matrix-isolation experiments.[14−16] However, PbH_3 can react with atomic H, and if the product is quenched immediately, PbH_4 should be stable enough to survive. We report here infrared spectra of PbH, PbH_2, and PbH_3 from the reaction of laser-ablated lead atoms with hydrogen molecules and atoms during condensation in excess argon, neon, and deuterium at 3.5 K. Complementary studies with tin and hydrogen give all four hydrides and are also included to compare with those of lead. Analogous work with Ge and H_2 gave the four hydrides and the novel Ge_2H_2 species.[17]

Experimental and Theoretical Methods

The laser-ablation matrix-isolation infrared spectroscopy experiment has been described previously.[18,19] Briefly, the Nd:YAG laser fundamental (1064 nm, 10 Hz repetition rate, 10 ns pulse width) was focused on a rotating lead (Alfa, 99.9999%) or tin (Alfa, 99.9999%) target using 1−5 mJ/pulse, and lead or tin atoms were codeposited with 4−15% H_2 (or D_2 or HD) in excess argon or neon or pure D_2 onto a 3.5 K CsI window. Infrared spectra were recorded after deposition, annealing, and UV−vis irradiation.

* To whom correspondence should be addressed. E-mail: lsa@virginia.edu.

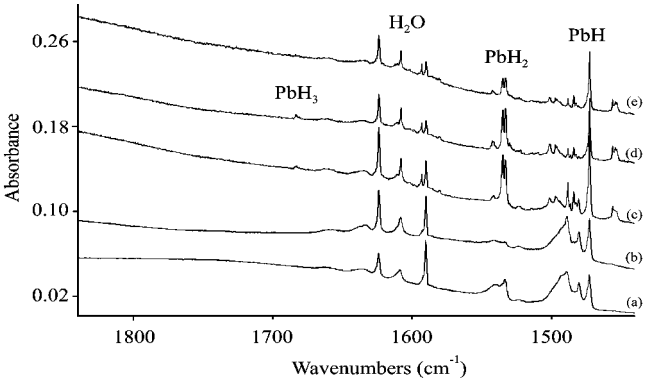

Figure 1. Infrared spectra in the 1840−1440 cm^{-1} region for laser-ablated lead codeposited with 10% H_2 in argon at 3.5 K: (a) after deposition, (b) after 290−700 nm photolysis, (c) after annealing to 25 K, (d) after annealing to 30 K, (e) after 240−700 nm photolysis.

Density functional theory frequency calculations were helpful in assigning palladium and platinum hydride spectra,[20,21] so similar B3LYP/6-311++G**/SDD calculations were performed for lead and tin hydrides.[22−25] Comparable results were obtained using the BPW91 functional and the LANL2DZ pseudopotential/basis. Although these calculations are only approximate, they provide a useful guide for assigning vibrational spectra.

Results and Discussion

Infrared spectra of lead and tin hydrides will be assigned on the basis of host matrix comparisons, isotopic substitution, and density functional theory frequency calculations.

Lead Hydrides. Infrared spectra for laser-ablated lead atom reaction products with H_2 and D_2 are compared in solid argon, neon, and deuterium at 3.5 K in Figures 1−3, and the new product absorptions are listed in Table 1. First note the strong PbH product bands with H_2 in neon at 1502.3 cm^{-1} and in argon at 1472.3 cm^{-1}, which shift for PbD to 1075.8 and 1055.3 cm^{-1} with D_2, and are not shifted with HD. The PbD molecule is observed at 1063.9 cm^{-1} in pure deuterium. The gas-phase fundamental[26] of PbH at 1504.6 cm^{-1} sustains a small 2.3 cm^{-1} red shift in neon and a larger 32.2 cm^{-1} red shift in solid argon, which are within the ranges observed for other molecules.[27] The H/D frequency ratios for each band, 1.396 and 1.395, are below

10.1021/jp025763i CCC: $22.00
Published on Web 06/11/2002

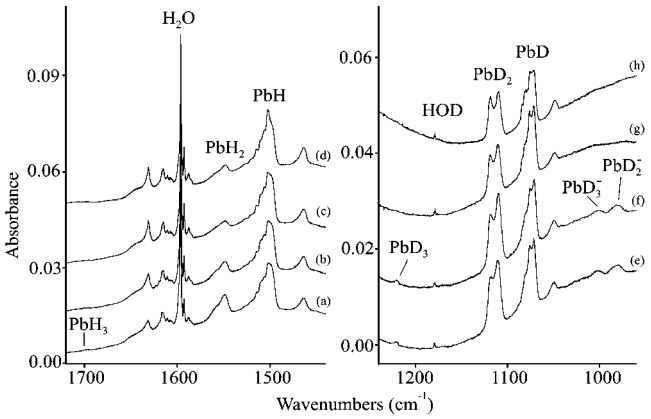

Figure 2. Infrared spectra for laser-ablated lead and isotopic hydrogen reaction products in solid neon at 3.5 K: (a) after deposition with 10% H_2 in neon, (b) after 380−700 nm photolysis, (c) after 290−700 nm photolysis, (d) after annealing to 7 K, (e) after deposition with 10% D_2 in neon, (f) after annealing to 7 K, (g) after 240−700 nm photolysis, (h) after annealing to 9 K.

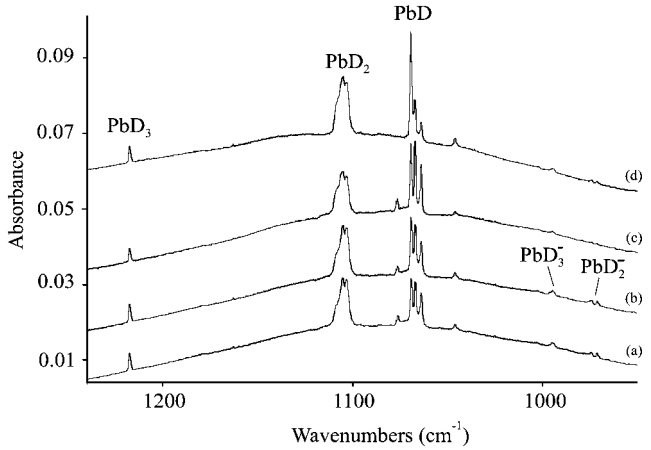

Figure 3. Infrared spectra for laser-ablated lead reaction products with pure deuterium at 3.5 K: (a) after deposition for 25 min, (b) after annealing to 6 K, (c) after 240−380 nm photolysis, (d) after annealing to 8 K.

the 1.410 harmonic PbH ratio by an amount appropriate for anharmonicity. Finally, the observed PbH frequency and bond length are in very good agreement with the results of our B3LYP and BPW91 calculations and two-configuration, two-component MRCIS calculations[28] (Table 2).

PbH is produced here in the endothermic reaction of lead atoms and H_2 where laser-ablated lead atoms contain sufficient excess energy[29] to drive reaction 1.

$$Pb + H_2 \rightarrow H + PbH \quad (\Delta E \geq 66.6 \text{ kcal/mol})^{26} \qquad (1)$$

Note site splittings on the PbH and PbD bands in each matrix including deuterium where PbD is trapped intermediate between the argon and neon matrix band positions. The logical source of site perturbations is unreacted H_2 as the extra features diminish at lower H_2 concentrations and on annealing, which allows H_2 to evaporate from the matrix. We note, however, that DFT calculations find the $(H_2)PbH$ complex to be unstable, in contrast to the analogous Pd and Pt species.[20,21] This is in accord with the survival of PbD in pure deuterium.

The new strong 1548.2 cm^{-1} band in neon shifts to 1532.7 cm^{-1} in argon, and both bands are reduced by the 1.394 factor for D_2 substitution to 1110.3 and 1099.3 cm^{-1}. These bands are not shifted in $H_2 + D_2$ experiments. In pure D_2 the analogous band appears at 1105.1 cm^{-1}. The 1548.2 cm^{-1} band is assigned to the antisymmetric stretching mode (ν_3, b_1) of PbH_2 in solid neon; the blue shoulder probably masks the weaker symmetric stretching mode (ν_1, a_1) calculated 2 cm^{-1} higher. After the strong 1502.3 cm^{-1} PbH band, the next strongest lead hydride feature, 1548.2 cm^{-1}, is appropriate for PbH_2, whose photodissociation is accompanied by the growth of PbH. The scale factor for the B3LYP frequency, 0.962, is nearly the same as that found for PtH_2, 0.973,[21] so the B3LYP calculation works almost as well for PbH_2.

TABLE 1: Infrared Absorptions (cm^{-1}) Observed for Reactions of Laser-Ablated Lead Atoms with Hydrogen and Deuterium

matrix	H_2	D_2	identification
Ne	1463.3	1048.4	late annealing pdt
Ar	1455.3	1043.7	late annealing pdt
D_2		1045.8	late annealing pdt
Ne	1521.6	1084.3	PbH, site
	1514.8	1081.6	PbH, site
	1509.8	1080.2	PbH, site
	1502.3	1075.8	PbH in neon
D_2		1076.2	PbD, site
		1069.2	PbD, site
		1066.8	PbD, site
		1063.9	PbD in deuterium
Ar	1488.2	1065.6	PbH, site
	1483.6	1062.4	PbH, site
	1479.9	1060.1	PbH, site
	1472.3	1055.3	PbH in argon
Ne	1559.6	1118.9	PbH_2
	1548.2	1110.3	PbH_2
D_2		1108.6	PbD_2
		1105.1	PbD_2
		1103.0	PbD_2
Ar	1534.6	1100.6	PbH_2
	1532.7	1099.3	PbH_2
Ar	1541.6	1106.4	PbH_2
Ne	1697.7	1220.2	PbH_3
D_2		1217.4	PbD_3
Ar	1683.8	1211.6	PbH_3
	1682.8		PbH_3
Ne	1400	1002	PbH_3^-
	1372	980	PbH_2^-
D_2		995	PbD_3^-
		973.9, 970.9	PbD_2^-

The direct insertion reaction 2 to form lead dihydride is exothermic. However, lead dihydride is photosensitive, reaction 3, but PbH_2 is re-formed on annealing to allow diffusion and reaction of H atoms, reaction 4.

$$Pb + H_2 \rightarrow PbH_2 \quad (\Delta E = -20.3 \text{ kcal/mol}) \qquad (2)$$

$$PbH_2 + \lambda > 240 \text{ nm} \rightarrow H + PbH \quad (\Delta E \geq 66.6 + 20.3 \geq 86.9 \text{ kcal/mol}) \qquad (3)$$

$$H + PbH \rightarrow PbH_2 \qquad (4)$$

Lead atoms in pure deuterium gave a sharp new 1217.2 cm^{-1} absorption, which had a weaker 1220.2 cm^{-1} counterpart in solid neon and shifted to 1697.7 cm^{-1} with H_2 substitution. Ultraviolet (240−380 nm) irradiation decreased the latter bands, the 1559.6 and 1548.2 cm^{-1} features, and increased the PbH absorptions. In the argon matrix, irradiation almost destroyed the 1534.6 and 1532.7 cm^{-1} bands and increased the PbH absorptions, but annealing to 25 K, which allowed the escape of H_2 and the diffusion of H atoms produced in the ablation process, increased the 1532.7 cm^{-1} band, and produced a new sharp 1683.8, 1682.8 cm^{-1} doublet. Similar behavior was found for D_2 in argon where

TABLE 2: Stretching Frequencies (cm^{-1}) and Bond Lengths Calculated at the DFT/6-311++G/SDD Level for Lead Hydrides**

	B3LYP[a]	BPW91[a,b]	other[c]	experimental[d]
PbH	1601.8, 1.843 Å	1567.5, 1.856 Å	1580, 1.830 Å	1564.1, 1.839 Å (gas)
($^2\Pi$)	(589)	(505)		1502.3, 1472.3 (Ne, Ar)
PbH_2	1605.0, 1603.3	1571.6, 1568.7	1745, 1753	1559.6, 1548.2 (Ne)
($^1A_1$)	(536), (624)	(537), (469)	(467), (433)	
	1.839 Å, 90.8°	1.851 Å, 90.3°	1.817 Å, 92.3°	1534.6, 1532.7 (Ar)
PbH_3	1775.0, 1703.6[e]	1732.1, 1647.4		1697.7 (Ne)
($^2A_1$)	(364 × 2), (56)	(317 × 2), (52)		1683.8 (Ar)
	1.769 Å, 109.1°			
PbH_4	1880.8, 1873.7	1828.0, 1815.3	1995, 1976	1823 (gas)
($^1A_1$)	(0), (268 × 3)	(242 × 3), (0)	(0), (225 × 3)	
	1.743 Å	1.753 Å	1.742 Å	
Pb_2H_2	1159.5, 1079.5, 865.7			
($^1A_1$)	(a_1, 49), (b_1, 201), (b_2, 349)			
	1.057 Å, 2.906 Å			
	H−Pb−H: 71.3°			
PbH_2^-	1345.7, 1334.2			1372 (Ne)
($^2B_1$)	(1099), (1389)			
	1.907 Å, 90.7°			
PbH_3^-	1384.7, 1372.9	1357.4, 1355.7		1400 (Ne)
($^1A_1$)	(a_1, 871), (e, 1289 × 2)	(a1, 790), (e, 1134 × 2)		
	1.891 Å, 91.6°	1.902 Å, 91.0°		

[a] This work, infrared intensities (km/mol) given in parentheses under the frequencies. [b] Strong absorptions using LANL2DZ were 16, 4, 23, and 25 cm^{-1} lower, respectively, for $PbH_{1,2,3,4}$. [c] For PbH, MRCIS, ref 28, and for PbH_2 and PbH_4, DHF, ref 7. [d] The first line for PbH is for the gas phase (ω_e), 1502.3 cm^{-1} (ν), ref 26; other entries are neon and argon matrix frequencies, respectively, this work. The first line for PbH_4 is for the gas phase, ref 3. [e] Stretching modes calculated for PbH_2D are 1775.0 (367), 1728.9 (172), and 1240.9 (116) cm^{-1}, for $PbHD_2$ they are 1752.2 (276), 1260.2 (181), and 1222.7 (69) cm^{-1}, and for PbD_3 they are 1259.4 (185 × 2), and 1205.8 (28) cm^{-1}. The values in parentheses are the infrared intensities (km/mol).

a new 1211.6 cm^{-1} band appeared on annealing. The diffusion of H(D) atoms at 20−30 K in solid argon is confirmed by the 2-fold increase in weak $HO_2(DO_2)$ absorptions[30] and the results of early ESR experiments on H atoms in solid argon.[31]

Complementary experiments were done with 4% H_2 and with 4% D_2 in argon subjected to microwave discharge during deposition, and the above-described PbH, PbH_2 and PbD, PbD_2 features were observed much the same. However, the sharp 1683.8, 1682.8 cm^{-1} doublet and 1211.6 cm^{-1} band appeared on annealing to 30 K with greater intensity than those of the undischarged precursor at the same concentration. Hence, it appears that diffusion and reaction of H or D atoms are responsible for this new product. Another experiment was performed using 10% $H_2 + D_2$ reagent in argon, and the $PbH_{1,2}$ and $PbD_{1,2}$ bands were observed as before. Annealing to 30−35 K produced the weak 1683.7 cm^{-1} band with new 1679.9 and 1660.1 cm^{-1} satellites and the 1211.6 cm^{-1} band with new 1212.8 and 1190.8 cm^{-1} satellites.

When one realizes that the symmetric stretching mode of PbH_3 is lower than the antisymmetric stretching mode, the position of frequencies for PbH_2D and $PbHD_2$ can be predicted (Table 2, footnote *e*). Accordingly the above new satellite features can be assigned to PbH_2D and $PbHD_2$, and the assignment of the 1683.8, 1682.8 cm^{-1} doublet (Figure 1) to PbH_3 radical follows. The B3LYP scale factor for the neon matrix counterpart, 0.945, is in line with the above scale factors for PbH and PbH_2. The plumbyl radical has not been detected previously, but it can reasonably be expected to follow in the CH_3, SiH_3, GeH_3, and SnH_3 radical series, whose ESR spectra have been observed in solid argon.[32]

The PbH_3 radical is thus made here on annealing by diffusion and reaction of H atoms in the solid matrixes. It comes as no surprise that the PbD_3 band is stronger in pure deuterium.

$$H + PbH_2 \rightarrow PbH_3 \qquad (5)$$

A major goal of this work was to prepare PbH_4, but reproducible bands are not observed in these experiments that are appropriate for assignment to PbH_4 or PbD_4, on the basis of our DFT calculations, scaled by our $PbH_{2,3}$ observations, and on the basis of the reported absorption of PbH_4 near 1820 cm^{-1}. Thus, we cannot confirm the recent gas-phase assignment[3] of PbH_4.

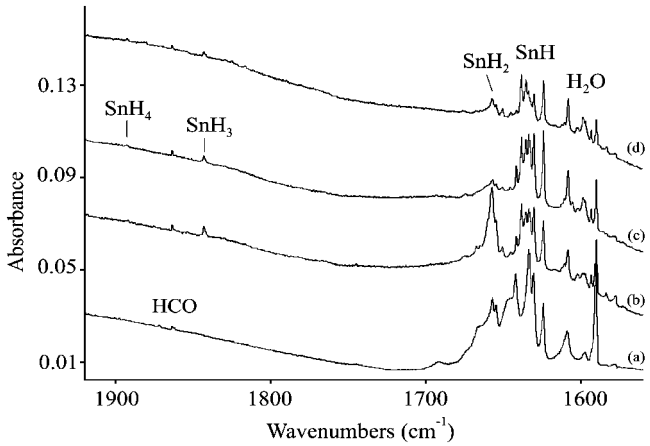

Figure 4. Infrared spectra in the 1920−1560 cm^{-1} region for laser-ablated tin codeposited with 10% H_2 in argon at 3.5 K: (a) after deposition, (b) after annealing to 25 K, (c) after 240−700 nm photolysis, (d) after annealing to 30 K.

Tin Hydrides. Infrared spectra for laser-ablated tin atom reaction products with hydrogen are compared in solid argon, neon, and deuterium at 3.5 K in Figures 4−6. The strong SnH bands at 1653.3 cm^{-1} in neon and at 1630.4 cm^{-1} with associated sites in solid argon shift to 1186.9 and 1169.5 cm^{-1} for SnD (Table 3). These bands are not changed in similar HD experiments. The SnD molecule absorbs strongly at 1183.1 and 1180.5 cm^{-1} in pure deuterium. The gas-phase SnH fundamental (1659.8 cm^{-1})[33] red shifts 4.5 cm^{-1} in solid neon and 29.4 cm^{-1} in solid argon. The H/D frequency ratios 1.395 and 1.395 are nearly the same as the ratios for PbH/PbD. The observed SnH frequencies are in good agreement with our DFT calculations and gas-phase fundamentals. Higher level calculations give higher frequencies.[34,35]

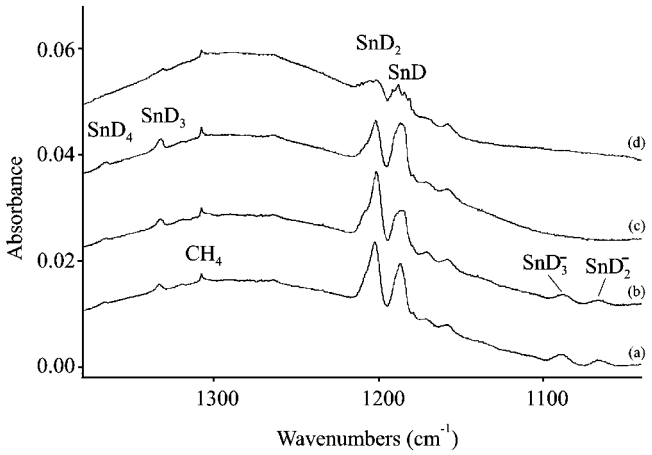

Figure 5. Infrared spectra for laser-ablated tin with 10% D_2 in neon at 3.5 K: (a) after sample deposition, (b) after annealing to 8 K, (c) after 240−380 nm photolysis, (d) after annealing to 11 K.

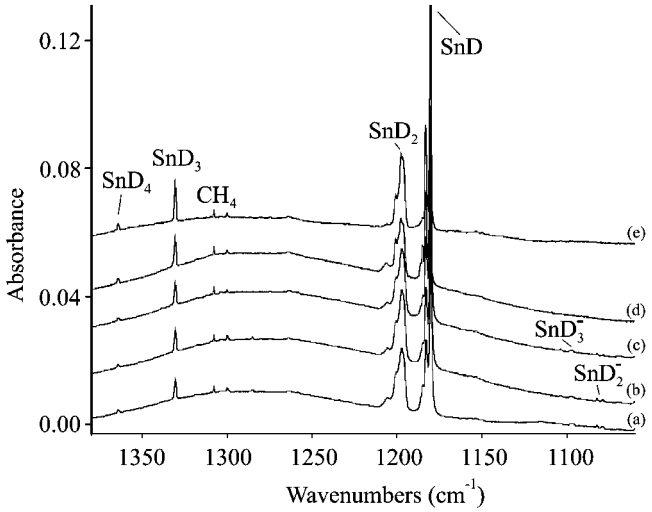

Figure 6. Infrared spectra for laser-ablated tin reaction products with pure deuterium at 3.5 K: (a) after deposition for 25 min, (b) after annealing to 7 K, (c) after 380−700 nm photolysis, (d) after 240−700 nm photolysis, (e) after 8 K annealing.

The site splittings on SnH and SnD absorptions and the observation of SnD in solid deuterium parallel the observations with lead. The next strongest absorptions at 1681.8 cm^{-1} in solid neon and 1654.8 cm^{-1} in solid argon are assigned to SnH_2, which has not been reported previously. These bands shift with D_2 substitution (1.399 and 1.392 H/D ratios), and intermediate 1200.7 and 1197.6 cm^{-1} bands are formed in pure deuterium. Our B3LYP calculation predicts ν_3 (b_1) and ν_1 (a_1) of SnH_2 at 1686.3 and 1699.9 cm^{-1}, respectively. The strong 1681.8 cm^{-1} neon matrix band is in excellent agreement with the 1686.3 cm^{-1} prediction. Both PbH_2 and SnH_2 are photosensitive: PbH and SnH increase on ultraviolet photolysis at the expense of PbH_2 and SnH_2, respectively.

Tin atoms in pure deuterium gave new bands at 1330.7 and 1364.4 cm^{-1}. Near agreement of the latter band with the ν_3 fundamental of SnD_4 in the gas phase[36] at 1367.5 cm^{-1} is compelling. Furthermore, our B3LYP calculation predicts this mode at 1369.6 cm^{-1}, which is also in excellent agreement. As for the other hydride species reported here, the neon and argon matrix counterparts, 1367 and 1359.9 cm^{-1}, bracket the deuterium matrix value. The 1904 and 1893.8 cm^{-1} absorptions for SnH_4 in solid neon and argon are in accord with the gas-phase ν_3 fundamental (1901.1 or 1905.8 cm^{-1}).[36,37]

TABLE 3: Infrared Absorptions (cm^{-1}) Observed for Reactions of Laser-Ablated Tin Atoms with Hydrogen and Deuterium

matrix	H_2	D_2	identification
Ne	1655.3	1186.9	SnH
D_2		1183.1	SnD
		1180.5	SnD
Ar	1641.9	1176.8	SnH, site
	1638.3	1175.5	SnH, site
	1633.5	1171.5	SnH, site
	1630.4	1169.5	SnH
Ne	1681.8	1201.8	SnH_2
D_2		1200.7	SnD_2
		1197.6	SnD_2
Ar	1657.3	1190.8	SnH_2
	1654.8	1188.2	SnH_2
Ne	1848.2	1333.1	SnH_3
D_2		1330.7	SnD_3
Ar	1843.2	1325.5	SnH_3
Ne	1904	1367	SnH_4
D_2		1364.4	SnD_4
Ar	1893.8	1359.9	SnH_4
Ne	1540	1088	SnH_3^- (ν_3, e)
	1506	1065	SnH_2^- (ν_1 and ν_3)
D_2		1097.4	SnD_3^- (ν_3, e)
		1082, 1078	SnD_2^- (ν_1 and ν_3)
Ne	1117.8		Sn_2H_2
	912.9	666.7	Sn_2H_2
	910.0	664.6	Sn_2H_2, site
D_2		668.1	Sn_2D_2, site
		665.3	Sn_2D_2
Ar	905		Sn_2H_2

The stronger new 1330.7 cm^{-1} band in pure deuterium is assigned here to the SnD_3 radical. Again, this band is bracketed by 1333.1 and 1325.5 cm^{-1} neon and argon matrix counterparts, which shift to 1848.2 and 1843.2 cm^{-1} with H_2 substitution. Our B3LYP calculation predicts the degenerate Sn−H stretching mode ν_3 (e) for SnH_3 at 1876.6 cm^{-1}, which is in excellent agreement. The stannyl radical has been observed in solid argon by ESR and the geometry deduced to be pyramidal.[32] Our DFT calculations find a 109.5° H−Sn−H bond angle for SnH_3 radical.

The $SnH_{1,2,3}$ hydrides are formed here in reactions analogous to those of the $PbH_{1,2,3}$ hydrides. An important difference is the larger yield of tin deuterides in pure deuterium as compared to lead deuterides (Figures 3 and 6). The SnD_3 band is stronger than the PbD_3 band, and SnD_4 is observed whereas PbD_4 is not detected (unless it falls under CH_4 near 1300 cm^{-1}). The latter is in accord with calculations of Dyall et al.[6] and the common chemical knowledge which find SnH_4 more stable than PbH_4. In contrast to plumbane, stannane can be formed by reaction 6.

$$MH_2 + H_2 \rightarrow MH_4 \qquad (6)$$

Sn_2H_2. The novel doubly bridged Si_2H_2 disilene has aroused a lot of interest because of the structure being different from that of linear C_2H_2.[38,39] The Si_2H_2 and Ge_2H_2 species were observed in laser-ablated Si and Ge experiments with H_2 in this laboratory.[17,40] The 912.9, 872.8, and 666.7 cm^{-1} bands with Sn and H_2, HD, and D_2 in excess neon are assigned to Sn_2H_2, Sn_2HD, and Sn_2D_2, respectively (Figure 7). The 912.9/666.7 = 1.369 ratio is less than that observed for terminal Sn−H/Sn−D stretching modes, which indicates greater anharmonicity for the motion of a bridged hydrogen. These bands increased slightly on 7 K annealing and decreased slightly on broad-band photolysis. First, only the 872.8 cm^{-1} band was observed with HD, and only the 912.9 and 666.7 cm^{-1} bands were found with a $H_2 + D_2$ mixture, which shows that one dihydrogen reagent

TABLE 4: Stretching Frequencies (cm^{-1}) and Bond Lengths Calculated at the DFT/6-311++G/SDD Level for Tin Hydrides**

	B3LYP[a]	BPW91[b]	other[c]	experimental[d]
SnH	1668.3, 1.791 Å	1622.5, 1.808 Å	1689, 1.815 Å	1718.4 (ωe, gas)
($^2\Pi$)	(583)	(515)	1725, 1.797 Å	1659.8 (ν, gas)
				1655.3 (Ne)
				1633.5 (Ar)
SnH_2	1699.9, 1686.3	1645.7, 1640.1	1874, 1867	1681.8 (Ne)
($^1A_1$)	(502), (567)	(458), (503)	(323), (411)	
	1.783 Å, 90.3°	1.800 Å, 189.7°		
SnH_3	1876.6, 1863.3	1827.2, 1799.4		
($^2A_1$)	(312 × 2), (28)	(280 × 2), (26)		
	1.721 Å, 109.5°	1.734 Å, 109.5°		
SnH_4	1962.5, 1926.9	1893.7, 1874.6	2069, 2047	1905.8 (gas)[d]
($^1A_1$)	(0), (240 × 3)	(0), (221 × 3)	(0), (166 × 3)	1904 (Ne)
	1.710 Å	1.723 Å		1893.8 (Ar)
Sn_2H_2	1279.8, 1176.3, 969.7			1117.8 (Ne)
($^1A_1$)	(a_1, 36), (b_1, 167), (b_2, 345)			912.9 (Ne)
	1.978 Å, 2.819 Å			
	H−Sn−H: 70.0°			
SnH_2^-	1453.1, 1435.6			1506 (Ne)
($^2B_1$)	(1193), (1365)			
	1.844 Å, 90.0°			
SnH_3^-	1516.9, 1492.0	1465.2, 1456.4		1540 (Ne)
($^1A_1$)	(a_1, 849), (e, 1240 × 2)	(a_1, 820), (e, 1125 × 2)		
	1.825 Å, 91.8°	1.843 Å, 91.1°		

[a] This work, infrared intensities (km/mol) given in parentheses under the frequencies. [b] Strong absorptions are 3, 4, 4, and 5 cm^{-1} lower for $SnH_{1,2,3,4}$, respectively, using the LANL2DZ pseudopotential/basis. [c] References 33−35 for SnH, ref 7 for SnH_2 and SnH_4. [d] Reference 37.

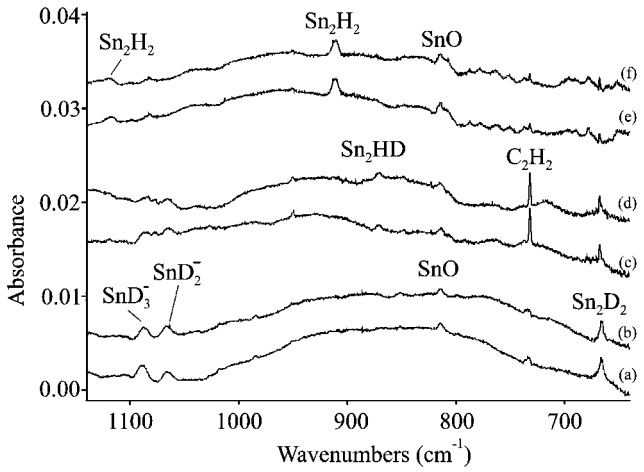

Figure 7. Infrared spectra in the 1140−640 cm^{-1} region for tin codeposited with isotopic hydrogen in neon at 3.5 K: (a) 10% D_2 in neon, (b) after annealing to 8 K, (c) 10% HD in neon, (d) after annealing to 8 K, (e) 10% H_2 in neon, (f) after annealing to 7 K.

molecule is involved. Unfortunately, only one stretching mode is strong for Sn_2HD. Second, our B3LYP calculations find a doubly bridged minimum-energy structure for Sn_2H_2 that is analogous to the structures calculated for Si_2H_2, Ge_2H_2, and Pb_2H_2.[17,38,39,41−44] This structure is found to be a local minimum but not viable energy-wise for C_2H_2.[45,46] Furthermore, our calculation predicts the strongest modes (b_2, antisymmetric Sn−H_2−Sn stretch) at 969.7 cm^{-1} for Sn_2H_2 (Table 4), at 919.1 cm^{-1} for Sn_2HD, and at 689.8 cm^{-1} for Sn_2D_2. This unusual isotopic pattern is matched by the observed bands (i.e., Sn_2HD is observed shifted 16.3% of the Sn_2H_2 to Sn_2D_2 separation, and the calculated position is 17.9%), and it arises from a change in the b_2 normal mode on symmetry lowering in the Sn_2HD "butterfly" species, as discussed for Ge_2H_2.[17] The computed structure of Sn_2H_2 is illustrated in Figure 8.[47]

In addition, our calculation finds the second strongest mode (b_1 antisymmetric Sn−H_2−Sn stretch) at 1176.3 cm^{-1}, and a band half as strong at 1117.8 cm^{-1} exhibits the same annealing

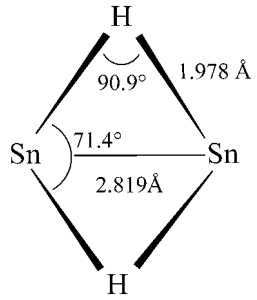

Figure 8. Structure calculated for Sn_2H_2 at the B3LYP/6-311++G**/SDD level.

and photolysis behavior. The observation of a second Sn_2H_2 mode strengthens this identification of Sn_2H_2: unfortunately, the position for Sn_2D_2 is masked by a weak SnO band at 814.2 cm^{-1} on the basis of the observation of SnO at 811 cm^{-1} in solid argon.[48] Our B3LYP calculation predicts two modes for doubly bridged Sn_2H_2 with similar scale factors, 0.941 and 0.950.

There are two favorable reactions to form Sn_2H_2 in these experiments, the dimerization of SnH, reaction 7, and the reaction of SnH_2 with Sn, reaction 8.

$$2SnH \rightarrow Sn_2H_2\,(^1A_1) \qquad (7)$$

$$SnH_2 + Sn \rightarrow Sn_2H_2\,(^1A_1) \qquad (8)$$

These reactions are both exothermic (B3LYP, −46.2 and −44.5 kcal/mol, respectively). Because no Sn_2H_2 was observed with the HD reagent, it is unlikely that reaction 7 makes a significant contribution to the yield of Sn_2H_2. The analogue of reaction 8 made most of the Ge_2H_2 observed previously.[17] Unfortunately, Pb_2H_2 was not detected in these experiments.

MH_3^- and MH_2^- Anions. Weak, broad 1540 and 1506 cm^{-1} bands with Sn and H_2 in neon become stronger 1088 and 1065 cm^{-1} absorptions with D_2 in neon. In pure deuterium the latter photosensitive bands were observed at 1097 and 1078, 1082 cm^{-1}. The latter bands were destroyed by $\lambda > 380$ nm photolysis

and the former by $\lambda > 240$ nm photolysis. Similar photosensitive absorptions were observed at 1837 and 1700 cm^{-1} for SiH_3^- and GeH_3^- in laser-ablation experiments,[17,40] and the 1540 cm^{-1} band is assigned accordingly to SnH_3^-. Our B3LYP calculation predicts the strongest ν_3 (e) mode at 1492.0 cm^{-1}, which is in reasonable agreement. The stronger 1506 cm^{-1} absorption is probably due to SnH_2^- calculated at 1435.6 and 1453.1 cm^{-1}, but we cannot be certain.

Similar weak, broad 1400 and 1372 cm^{-1} bands with Pb and H_2 in neon became stronger 1002 and 980 cm^{-1} absorptions with D_2 in neon (Figure 2). In pure deuterium the latter bands appeared at 995 and 973.9, 970.9 cm^{-1}, which is the typical neon-to-deuterium matrix shift, and the doublet was destroyed and the 995 cm^{-1} band decreased by UV light (Figure 3). The 1372 cm^{-1} band was decreased by $\lambda > 380$ nm and destroyed by $\lambda > 290$ nm mercury arc radiation. The 1372/980 = 1.400 H/D isotopic ratio is appropriate for a terminal Pb−H/Pb−D vibrational mode. Our B3LYP calculation predicts the stretching modes for PbH_2^- anion at 1345.7 and 1334.2 cm^{-1}, which are lower than the broad 1372 cm^{-1} absorption. In the pure deuterium matrix the counterpart is split at 973.9 and 970.9 cm^{-1}. These bands are assigned to PbH_2^-, which is more photosensitive than PbH_3^-. The weaker 1400 cm^{-1} band is probably due to the stronger ν_3 (e) mode calculated at 1372.9 cm^{-1} for PbH_3^-. The DFT frequencies are lower than the observed frequencies for Sn and Pb hydride anions, and Ge hydride anions as well,[17] but the reverse relationship is found for Si hydride anions.[40]

The metal trihydride anions have been considered in the exothermic decomposition of MH_5^- anions, and PbH_3^- has been employed as a model for chemical shifts.[49,50] The MH_3^- anions are made here from the capture of laser-ablated electrons by the MH_3 radical product as found for SiH_3^- and GeH_3^- in similar studies.[17,40] These MH_3^- anions are stable as the electron-capture process is exothermic by 33.1, 35.3, 39.3, and 47.5 kcal/mol for Si, Ge, Sn, and Pb, respectively, at the B3LYP level (BPW91 results are 0.8−1.5 kcal/mol less). We suggest that SnH_3^- and PbH_3^- should be observable under gas-phase discharge conditions.

$$MH_3 + e^- \rightarrow MH_3^- \quad (9)$$

A similar process forms the dihydride anions. We note, however, the opposite trend in MH_2^- stabilities with increasing M size: the electron-capture process is exothermic by 27.2, 21.0, 22.4, and 14.8 kcal/mol for the closed-shell MH_2 species of Si, Ge, Sn, and Pb, respectively, at the B3LYP level. The anion M−H bonds are 4−7% longer for Pb and 3−6% longer for Sn, but there is a substantial reduction in the pyramidal angle for MH_3 upon electron capture and little change in the MH_2 valence angle.

$$MH_2 + e^- \rightarrow MH_2^- \quad (10)$$

Reactivities of Si, Ge, Sn, and Pb. Laser-ablated tin and lead atoms react with H_2 much the same way as silicon and germanium atoms,[17,40] but there are some trends in reactivities. As predicted earlier,[6,7] the exothermicity of reaction 6 decreases from Si to Ge to Sn, and the reaction becomes endothermic for Pb. This is demonstrated in Figure 9, which compares spectra of laser-ablated Si, Ge, Sn, and Pb reaction products in pure deuterium. No SiD_2 is trapped, and the yield of SiD_4 is huge; however, GeD_2 and SnD_2 are trapped along with small amounts of GeD_4 and SnD_4. Although PbD_2 is observed, we find no evidence for PbD_4, consistent with the endothermic nature of reaction 6 for lead.

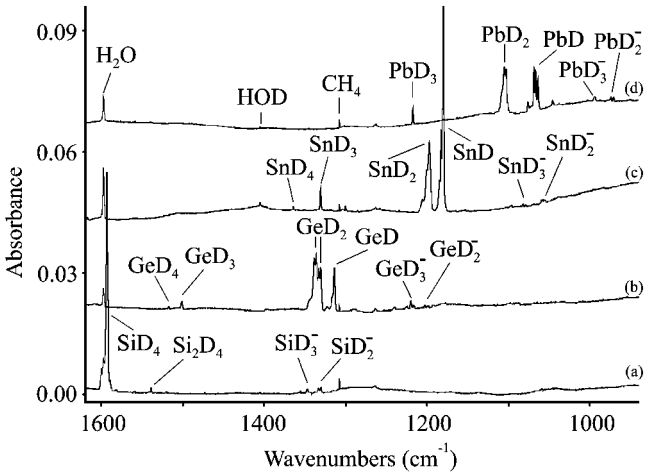

Figure 9. Infrared spectra in the 1620−940 cm^{-1} region for laser-ablated Si, Ge, Sn, and Pb codeposited with pure deuterium for 25 min at 3.5 K: (a) Si, (b) Ge, (c) Sn, (d) Pb.

Note that SiD is not trapped in pure deuterium as reaction to form SiD_3 is favorable (SiD_3 is masked by SiD_4 at 1593 cm^{-1} but observed at 668.7 and 545.7 cm^{-1} in other regions of the spectrum), but GeD, SnD, and PbD are trapped along with GeD_3, SnD_3, and PbD_3.

Similar yields of photosensitive bands were observed with all four metals for MD_3^- and MD_2^- anions. Even though SiD_2 reacts with D_2 to form SiD_4, SiD_2^- does not react likewise as SiD_4^- is unstable.[40,51]

Conclusions

Laser-ablated Sn atoms and H_2 molecules in excess neon and argon react during condensation to produce $SnH_{1,2,3,4}$ as identified from infrared spectra with D_2 and HD substitution, and from agreement with frequencies calculated by density functional theory. The novel ditin species Sn_2H_2 is also formed in further reactions. The $PbH_{1,2,3}$ intermediates are produced in analogous experiments, but we find no evidence for PbH_4. All four tin deuterides and the first three lead deuterides are observed in pure deuterium. In this work, we report the first infrared spectra of the reactive $SnH_{2,3}$ and $PbH_{2,3}$ species. Evidence is also presented for the photosensitive MH_3^- and MH_2^- anions formed through electron-capture processes.

Acknowledgment. We gratefully acknowledge support for this work from the NSF (Grant CHE 00-78836), several argon matrix experiments performed by B. Liang, and helpful correspondence with K. Faegri and P. Pyykkö.

References and Notes

(1) Cotton, F. A.; Wilkinson, G.; Murillo, C. A.; Bochmann, M. *Advanced Inorganic Chemistry*, 6th ed.; Wiley: New York, 1999.
(2) Saalfeld, F. E.; Svec, H. J. *Inorg. Chem.* **1963**, *2*, 46.
(3) Krivtsum, V. M.; Kuritsyn, Yu. A.; Snegirev, E. P. *Opt. Spectrosc.* **1999**, *86*, 686.
(4) Desclaux, J. P.; Pyykkö, P. *Chem Phys. Lett.* **1974**, *29*, 534.
(5) Schwerdtfeger, P.; Silberbach, H.; Miehlich, B. *J. Chem. Phys.* **1989**, *90*, 762.
(6) Dyall, K. G.; Taylor, P. R.; Faegri, K.; Partridge, H. *J. Chem. Phys.* **1991**, *95*, 2583.
(7) Dyall, K. G. *J. Chem. Phys.* **1992**, *96*, 1210.
(8) Schwerdtfeger, P.; Heath, G. A.; Dolg, M.; Bennett, M. A. *J. Am. Chem. Soc.* **1992**, *114*, 7518.
(9) Kaupp, M.; Schleyer, P. v. R. *J. Am. Chem. Soc.* **1993**, *115*, 1061.

(10) Visser, O.; Visscher, L.; Aerts, P. J. C.; Nieuwpoort, W. C. *Theor. Chim. Acta* **1992**, *81*, 405.
(11) Barandiaran, Z.; Seijo, L. *J. Chem. Phys.* **1994**, *101*, 4049.
(12) Wang, S. G.; Schwarz, W. H. E. *J. Mol. Struct.: THEOCHEM* **1995**, *338*, 347.
(13) Han, Y.-K.; Bae, C.; Lee, Y. S. *J. Chem. Phys.* **1999**, *19*, 9353.
(14) Chertihin, G. V.; Andrews, L. *J. Am. Chem. Soc.* **1995**, *117*, 6402.
(15) Chertihin, G. V.; Andrews, L. *J. Phys. Chem.* **1995**, *99*, 15004.
(16) Siegbahn, P. E.; Blomberg, M. R. A.; Svensson, M. *J. Am. Chem. Soc.* **1993**, *115*, 4191. In contrast the $ZrH_2 + H_2 \rightarrow ZrH_4$ reaction is calculated to be exothermic by 41 kcal/mol.
(17) Wang, X.; Andrews, L.; Kushto, G. P. *J. Phys. Chem. A* **2002**, *106*, 5809.
(18) Hassanzadeh, P.; Andrews, L. *J. Phys. Chem. A* **1992**, *96*, 9177.
(19) Chertihin, G. V.; Andrews, L. *J. Chem. Phys.* **1996**, *105*, 2561.
(20) Andrews, L.; Manceron, L.; Alikhani, M. E.; Wang, X. *J. Am. Chem. Soc.* **2000**, *122*, 11011.
(21) Andrews, L.; Wang, X.; Manceron, L. *J. Chem. Phys.* **2001**, *114*, 1559.
(22) Frisch, M. J.; Trucks, G. W.; Schlegel, H. B.; Scuseria, G. E.; Robb, M. A.; Cheeseman, J. R.; Zakrzewski, V. G.; Montgomery, J. A., Jr.; Stratmann, R. E.; Burant, J. C.; Dapprich, S.; Millam, J. M.; Daniels, A. D.; Kudin, K. N.; Strain, M. C.; Farkas, O.; Tomasi, J.; Barone, V.; Cossi, M.; Cammi, R.; Mennucci, B.; Pomelli, C.; Adamo, C.; Clifford, S.; Ochterski, J.; Petersson, G. A.; Ayala, P. Y.; Cui, Q.; Morokuma, K.; Malick, D. K.; Rabuck, A. D.; Raghavachari, K.; Foresman, J. B.; Cioslowski, J.; Ortiz, J. V.; Stefanov, B. B.; Liu, G.; Liashenko, A.; Piskorz, P.; Komaromi, I.; Gomperts, R.; Martin, R. L.; Fox, D. J.; Keith, T.; Al-Laham, M. A.; Peng, C. Y.; Nanayakkara, A.; Gonzalez, C.; Challacombe, M.; Gill, P. M. W.; Johnson, B. G.; Chen, W.; Wong, M. W.; Andres, J. L.; Head-Gordon, M.; Replogle, E. S.; Pople, J. A. *Gaussian 98*, revision A.7; Gaussian, Inc.: Pittsburgh, PA, 1998.
(23) (a) Becke, A. D. *J. Chem. Phys.* **1993**, *98*, 5648. (b) Lee, C.; Yang, W; Parr, R. G. *Phys. Rev. B* **1988**, *37*, 785.
(24) (a) Krishnan, R.; Binkley, J. S.; Seeger, R.; Pople, J. A. *J. Chem. Phys.* **1980**, *72*, 650. (b) Frisch, M. J.; Pople, J. A.; Binkley, J. S. *J. Chem. Phys.* **1984**, *80*, 3265.
(25) Andrae, D.; Haussermann, U.; Dolg, M.; Stoll, H.; Preuss, H. *Theor. Chim. Acta* **1990**, *77*, 123.
(26) Herzberg, G.; Huber, K. P. *Constants of Diatomic Molecules*; Van Nostrand Reinhold: New York, 1979.
(27) Jacox, M. E. *Chem. Phys.* **1994**, *189*, 149.
(28) Metz, B.; Stoll, H.; Dolg, M. *J. Chem. Phys.* **2000**, *113*, 2563.
(29) Kang, H.; Beauchamp, J. L. *J. Phys. Chem.* **1985**, *89*, 3364.
(30) Smith, D. W.; Andrews, L. *J. Chem. Phys.* **1974**, *60*, 81.
(31) Foner, S. N.; Cochran, E. L.; Bowers, V. A.; Jen, C. K. *J. Chem. Phys.* **1960**, *32*, 963.
(32) Morehouse, R. L.; Christiansen, J. J.; Gordy, W. *J. Chem. Phys.* **1966**, *45*, 1751.
(33) Zimmermann, W.; Simon, U.; Petri, M.; Urban, W. *Mol. Phys.* **1991**, *74*, 1287.
(34) Alekeyev, A. B.; Liebermann, H.-P.; Buenker, R. J.; Hirsch, G. *Mol. Phys.* **1996**, *88*, 591.
(35) Chapman, D. A.; Balasubramanian, K.; Lin, S. H. *J. Chem. Phys.* **1988**, *88*, 3826.
(36) Levin, I. W.; Ziffer, H. *J. Chem. Phys.* **1965**, *43*, 4023.
(37) Halonen, M.; Halonen, L.; Bürger, H.; Sommer, S. *J. Phys. Chem.* **1990**, *94*, 5222.
(38) Colegrove, B. T.; Schaefer, H. F., III *J. Phys. Chem.* **1990**, *94*, 5593 and references therein.
(39) Hühn, M. M.; Amos, R. D.; Kobayashi, R.; Handy, N. C. *J. Chem. Phys.* **1993**, *98*, 7107.
(40) Andrews, L.; Wang, X. *J. Phys. Chem. A*, accepted.
(41) Palágyi, Z.; Schaefer, H. F., III; Kapuy, E. *J. Am. Chem. Soc.* **1993**, *115*, 6901.
(42) Boone, A. J.; Magers, D. H.; Leszczynski, J. *Int. J. Quantum Chem.* **1998**, *70*, 925.
(43) Ricca, A.; Bauschlicher, C. W., Jr. *J. Phys. Chem. A* **1999**, *103*, 11121.
(44) Chen, Y.; Hartmann, M.; Diedenhofen, M.; Frenking, G. *Angew. Chem., Int. Ed.* **2001**, *40*, 2052.
(45) Brinkley, J. S. *J. Am. Chem. Soc.* **1984**, *106*, 603.
(46) Schleyer, P. v. R. *J. Phys. Chem.* **1990**, *94*, 5560.
(47) Although Sn_2H_2 is observed in these experiments, we did not detect the magneto-infrared bands reported for Sn_2 in solid matrixes; see: Li, S.; Van Zee, R. J.; Weltner, W., Jr. *J. Chem. Phys.* **1994**, *100*, 7079.
(48) Ogden, J. S.; Ricks, M. J. *J. Chem. Phys.* **1970**, *53*, 896.
(49) Moc, J. *J. Mol. Struct.: THEOCHEM* **1999**, *461*−*462*, 249.
(50) Edlund, U.; Lejon, T.; Pyykkö, P.; Venkatachalam, T. K.; Buncel, E. *J. Am. Chem. Soc.* **1987**, *109*, 5982.
(51) Pak, C.; Rienstra-Kiracofe, J. C.; Schaefer, H. F., III. *J. Phys. Chem. A* **2000**, *104*, 11232.